Journal of Applied Polymer Science

Ab Initio Emulsion RAFT Polymerization of Vinylidene Chloride Mediated by Amphiphilic Macro-RAFT Agents

Jie Yang, Yongzhong Bao, Pengju Pan
State Key Laboratory of Chemical Engineering, Department of Chemical and Biological Engineering, Zhejiang University, Hangzhou 310027, China
Correspondence to: Y. Bao (E-mail: yongzhongbao@zju.edu.cn)

ABSTRACT: An amphiphilic copolymer poly(acrylic acid)-*block*-poly(styrene) (PAA-*b*-PS) with a trithiocarbonate reactive group was used in the *ab initio* reversible addition-fragmentation chain transfer (RAFT) emulsion polymerization of vinylidene chloride (VDC). The fast polymerization and high conversion were achieved. The parameters for a good control over the formation of well-defined PAA-*b*-PS-*b*-PVDC amphiphilic block copolymers and self-stabilized latexes were identified. To improve the emulsion stability and prevent the desorption of water-soluble initiating radicals, the acid groups of PAA-*b*-PS were neutralized by NaOH at the later stage of polymerization. The PAA-*b*-PS-*b*-PVDC block copolymer with a high molar mass of 30 kg mol^{-1} and the stable latex with 30 wt % solid content was obtained. The kinetics of RAFT emulsion copolymerization of VDC in a living manner was first investigated. The as-prepared PAA-*b*-PS-*b*-PVDC latex particles were further used as seeds in the emulsion polymerization of styrene, enabling the preparation of novel PAA-*b*-PS-*b*-PVDC-*b*-PS tetra-block copolymers with a molar mass of 76 kg mol^{-1} and a relatively low molecular weight distribution of 1.6. © 2014 Wiley Periodicals, Inc. J. Appl. Polym. Sci. **2014**, *131*, 40391.

KEYWORDS: copolymers; emulsion polymerization; kinetics

Received 11 October 2013; accepted 4 January 2014
DOI: 10.1002/app.40391

INTRODUCTION

Poly(vinylidene chloride) (PVDC) has excellent barrier properties toward gases and water vapor and has been widely used in the food and pharmaceutical packaging industry.[1,2] Commercial PVDC, usually containing a small percentage of comonomer (typically methyl acrylate, vinyl chloride, or acrylonitrile), is produced by the conventional free-radical suspension and emulsion polymerizations. The PVDC latex prepared by the emulsion polymerization is usually coated onto the plastic films or paper sheets to improve their barrier properties. Because of the significant chain transfer reaction from the growing macromolecular radicals to VDC monomer, VDC polymers prepared by the conventional free radical polymerization exhibit the structural defects and poor thermal stability.[3–5] Moreover, the PVDC latex usually shows even lower thermal stability than the PVDC powder prepared by the suspension polymerization,[4,6,7] due to the presence of a greater amount of emulsifier and other additives accelerating the polymer degradation. During the storage of PVDC latex, the hydrogen chloride produced by thermal degradation of PVDC and formation of oxygen-containing defect structures would lead to the coloration and coagulation of latex.[7,8] Conversely, the emulsifier existed in the latex would transfer into the VDC polymer film after coating. Further migration of emulsifier from the coating to matrix would decrease the barrier properties of coated packaging materials. Therefore, the preparation of VDC polymer latex with well-defined molecular structure and free of emulsifier is essential for their practical applications.

The kinetics and mechanism of VDC emulsion (co)polymerization have been investigated by several researchers.[9–11] Yu et al.[9] found that the critical conversion at the end of Interval 2 in the emulsion copolymerization of VDC was about 60%, and the comonomer type had no great effect on the copolymerization rate and intrinsic viscosity of a VDC copolymer. Nomura et al.[10,11] studied the kinetic behavior of the emulsion (co)polymerization of VDC at 50°C using sodium lauryl sulfate as the emulsifier and potassium persulfate as the initiator, respectively, and established the equations relating the number of polymer particles and polymerization rate to the initial initiator and emulsifier concentrations.

The controlled radical polymerizations including nitroxide-mediated polymerization, atom transfer radical polymerization, reversible addition-fragmentation chain transfer (RAFT) polymerization, and iodine transfer polymerization have received much attention due to their good controllability over the chain microstructures such as the molecular weight, molecular weight distribution, and composition.[12–17] Among these methods, RAFT

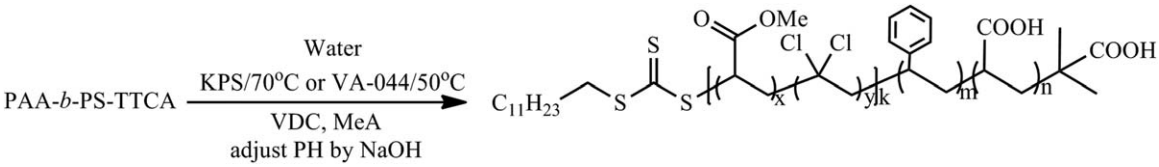

Scheme 1. Synthetic route for RAFT emulsion copolymerization of VDC and MeA.

polymerization shows good controllability for the polymerization of a wide variety of monomers under the mild conditions. However, few works have been focused on the synthesis of VDC-based polymers via RAFT polymerization. Severac et al.[18] pioneered a work on RAFT copolymerization of VDC and methyl acrylate (MeA) using ditiobenzoates as the chain transfer agents (CTAs). Lately, the preparation of phosphonated VDC copolymer and CeO_2/PVDC hybrid latex via RAFT copolymerization was reported by the same group.[19,20] Velasquez et al.[21] synthesized the VDC–MA and VDC–acrylic acid (AA) copolymers by RAFT polymerization using a trithiocarbonate CTA, and obtained the PVDC-based amphiphilic block copolymers using the hydrophobic poly(VDC-*co*-MeA) and hydrophilic PAA macromolecular RAFT agents. However, the living emulsion (co)polymerization of VDC free of emulsifiers has not been explored.

Ab initio emulsion RAFT polymerization provides a novel approach to prepare polymer latex with fast polymerization rate, high colloidal stability, controllable molecular weight, and low polydispersity (PDI). Previous studies on *ab initio* emulsion RAFT polymerization were mainly focused on styrene or acrylate monomer.[22–24] Wang et al.[24] found that the block lengths of amphiphilic poly(acrylic acid-*b*-styrene) (PAA-*b*-PS) trithiocarbonate macro-RAFT agent and the neutralization of poly(acrylic acid) play a key role on the colloidal stability and molecular weight in the *ab initio* emulsion polymerization of styrene. The neutralization of PAA increased the colloidal stability but led to low controllability of molecular weight and broad molecular weight distribution. Post-addition of NaOH was effective to improve the stability of latex system. The butadiene homopolymerization and copolymerization of methyl-methylene-butyrolactone and styrene were also successfully performed via the *ab initio* RAFT emulsion polymerization technique by the same group.[25,26]

In this article, we developed a method to prepare VDC copolymer with high, controlled molecular weight (>25 kg mol^{-1}) and well-defined structure via the surfactant-free *Ab initio* RAFT emulsion polymerization using the amphiphilic poly(acrylic acid-*b*-styrene) macro-RAFT agent. Methyl acrylate (MeA) was chosen as the comonomer as it is commonly used in PVDC modification and has a near copolymerization reactivity ratio to VDC ($r_{VDC} = 1.0$, $r_{MA} = 1.0$).[7] Effects of the macro-RAFT structure and concentration on the colloidal stability, kinetics, and controllability of polymerizations were investigated. The controlled polymerization was further expanded to the seeded emulsion polymerization of styrene.

EXPERIMENTAL

Materials

VDC was purchased from Zhejiang Juhua (Quzhou, China) and purified by distillation twice under a N_2 protection. Methyl acrylate (MeA), acrylic acid (AA), and styrene (St) were purchased from Sinopharm Chemical Reagent (SCRC, Shanghai, China) and purified by distillation under vacuum. 2,2′-Azobis (isobutyronitrile) (AIBN, 98%) was purchased from SCRC and purified by recrystallization in ethanol. 2,2′-Azobis[2-(2-imidazolin-2-yl)propane]dihydrochloride (VA044, >99%), potassium persulfate (KPS, >99%), and sodium hydroxide (NaOH, >96%) with analytical purity were purchased from J&K Chemical Reagent and used as received. 1,4-Dioxane (99%) and tetrahydrofuran (THF, 99%) purchased from SCRC were dried with CaH_2 and then distilled before using. The RAFT agent 2-(dodecylthiocarbonothioylthio)-2-methylpropionic acid (TTCA) was synthesized according to the method reported by Lai et al.[27]

Synthesis of Macro-RAFT Agents

The macro-RAFT agents were labeled as PAA_x-*b*-PS_y-TTCA, where *x* and *y* correspond to the polymerization degrees of PAA and PS blocks, respectively. The macro-RAFT agents PAA_{30}-*b*-PS_5-TTCA were synthesized as follows. 4.27 g (11.7 mmol) of TTCA, 0.192 g (1.17 mmol) of AIBN, and 25.0 g (347.2 mmol) of AA were dissolved in 80 mL of dioxane and were then introduced to a flask. The reaction was allowed to proceed at 80°C for 6h under stirring. The flask was then cooled to room temperature and the other solution containing 11.71 g (112.6 mmol) of styrene, 0.192 g (1.17 mmol) of AIBN, and 20 mL of dioxane was added. The mixture was deoxygenated and reacted for further 12 h at 80°C. The macro-RAFT agents were collected by precipitation twice in diethyl ether, followed by drying under vacuum at 80°C.

Ab Initio Emulsion Polymerization of VDC

The conditions of *ab initio* emulsion copolymerization of VDC using macro-RAFT agent as both the surfactant and RAFT agent are shown in Scheme 1.

A typical polymerization procedure was as follows. 3.00 g (1.0 mmol) of PAA-*b*-PS-TTCA RAFT agent was dissolved in 270 g of deionized water. Then, 30.0g monomers with a VDC/MeA mass ratio of 9 : 1 were added and mixed with the aqueous solution in a 1000 mL autoclave. The autoclave was sealed and immersed in an ice water (0°C) bath. After replacing air in the reactor with nitrogen for 30 min, the temperature of the reactor was increased to 70°C. 0.057 g (0.212 mmol) of KPS initiator dissolved in 30 mL deionized water was injected into the reactor to start the polymerization. After a certain time interval, samples were withdrawn for the various measurements.

Seeded RAFT Emulsion Polymerization of Styrene

Before the seeded emulsion polymerization, the seed latexes were bubbled by nitrogen to remove the unreacted VDC monomer. Then, 7.863 g styrene was introduced into 50.0 g the seed latexes, and the mixture was stirred overnight at 0°C in a three-

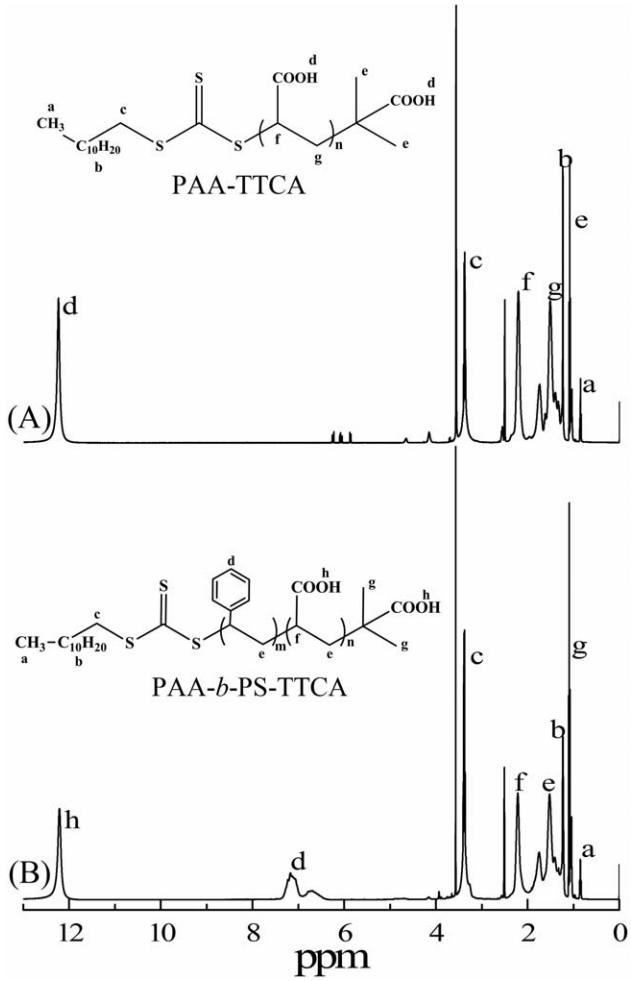

Figure 1. ^{1}H-NMR spectra of PAA–TTCA (A) and PAA-*b*-PS-TTCA diblock copolymer (B).

neck round-bottomed flask to ensure a full swelling of styrene into the seed particles. The polymerization was started by raising temperature to 50°C and adding of a water solution of VA044 0.086 g. The polymerization was allowed to proceed at 50°C for 10 h. The latex sample was withdrawn for the transmission electron microscopy (TEM), dynamic light scattering (DLS), and gel permeation chromatography (GPC) analysis.

Characterization

The structure of macro-RAFT agents was determined on a Bruker Avance 500M ^{1}H-NMR (Billerica) spectrometer using DMSO as the solvent.

The pH value of aqueous phase was probed by a pH-meter (LEICI PHS-2C) using a micro-pH electrode (E201-4). The critical micelle concentration of the macro-RAFT agent in water was measured by conductimetry at 30°C.

The *Z*-average diameter (D_z) and polydispersity factor (σ) were measured on a Malvern ZETASIZER 3000 HAS instrument at 25°C by DLS at an angle of 90°.

For the TEM measurement, the samples were dried in vacuum at 30°C for 2 h to remove the residual VDC monomer. Diluted samples were dropped on a carbon-coated copper grid and dried under ambient conditions. The morphology of latex particles was observed on a TEM (JEOL JEM 1230 electron microscope) operated at a voltage of 80 kV.

The average molecular weight and molecular weight distribution of polymers were measured using a Waters 1525/2414 GPC system (Waters, Milford) equipped with Waters Styragel® columns HR 4, 3, 1, and refractive index detector. THF was used as the eluent at a flow rate of 1 mL min^{-1}. Polystyrene samples with narrow molecular weight distributions were used as standards to obtain the calibration curve (molar mass range, 162–2,906,580 g mol^{-1} for columns HR 4, 3, and 1).

RESULTS AND DISCUSSION

Synthesis and Characterization of Macro-RAFT Agents

PAA–TTCA and PAA-*b*-PS-TTCA macro-RAFT agents were synthesized by the RAFT solution polymerization of AA and sequentially solution polymerization of styrene, respectively. The number-average molar weights (M_n^{GPC}) of PAA–TTCA and PAA-*b*-PS-TTCA macro-CTAs determined by GPC were 2525 and 3145 g mol^{-1}, respectively, consistent well with the designed molar weights. PAA–TTCA and PAA-*b*-PS-TTCA exhibited narrow molecular weight distributions with the polydispersity values around 1.20, evidencing the living nature of AA and styrene polymerizations. The structures of PAA–TTCA and PAA-*b*-PS-TTCA macro-RAFT agents were analyzed by ^{1}H-NMR and their spectra are shown in Figure 1.

^{1}H-NMR signals of PAA–TTCA were assigned as in Figure 1(A) (in ppm): 0.85 (3H, —CH_3 of —$C_{12}H_{25}$ chain moiety), 1.24 (18H, —$CH_2(CH_2)_9CH_3$ of —$C_{12}H_{25}$ chain), 1.52 (—C—CH_2—C— of PAA chain), 2.20 (1H, —CH(COOH) — of PAA chain), and 12.2 (1H, —COOH of PAA chain).

^{1}H-NMR signals of PAA-*b*-PS-TTCA were assigned as follows (in ppm): 0.84 (3H, —CH_3 of —$C_{12}H_{25}$ chain moiety), 1.03 (3H, —CH_3 of — $(CH_3)_2$— (COOH) chain moiety), 1.25 (18H, —$CH_2(CH_2)_9CH_3$ of —C_{12}—H_{25} chain), 1.56 (—C—CH_2—C— of PAA-*b*-PS chain), 2.24 (—CH(COOH) — of PAA chain), 7.18 (—Ph—H of PS chain), and 12.6 (—COOH of PAA chain). The peak areas of the signal at 0.84 ppm (0.899, 3H, —CH_3 of —$C_{12}H_{25}$ chain moiety), the signal at 7.18 ppm (8.533, 5H, —Ph—H of PS chain), and the signal at 12.6 ppm (10.167, 1H, —COOH of PAA and TTCA moiety) were used to estimate the copolymer composition, and it was calculated that PAA-*b*-PS-TTCA approximately contained 30 acrylic acid units and 5 styrene units. The M_n of PAA-*b*-PS-TTCA determined from the ^{1}H-NMR analysis was about 3000 g mol^{-1}.

Because of the coexistence of hydrophilic and hydrophobic blocks, PAA-*b*-PS-TTCA macro-RAFT agent might form aggregates in water. The critical micelle concentration of non-neutralized PAA-*b*-PS-TTCA macro-RAFT agent, determined by conductimetry at 25°C, was 0.88 mmol L^{-1}, which is far below the aqueous concentration of PAA-*b*-PS-TTCA macro-RAFT agent used in this work. Thus, the micelles would be existed and the micelle nucleation would be the main nucleation mode for the emulsion copolymerization of VDC and MeA.

Table I. Conditions for *Ab Initio* RAFT Emulsion Copolymerization of VDC and MeA Using Macro-RAFT Agent (pH Adjusted with NaOH)[a]

Entry	$[M]_0/[CTA]_0$	Monomers (%)[b]	$[CTA]_0$ (mmol L_{aq}^{-1})	$pH_{initi.}/pH_{end}$	$[OH^{-1}]/[-COOH]$	Time (min)	Conv. (%)	$M_{n,th}$ (g mol^{-1})	$M_{n,GPC}$ (g mol^{-1})	PDI	D_z (nm)[c]	σ[c]
E1	276	10	4.2	6.4/5.7	0.6	570	73	22,550	26,820	3.62	78	0.25
E2[d]	295	10	3.9	3.0/2.0	0.0	330	-	-	19,490[d] 20,650[d]	1.55 1.69	103 -	0.41 -
E3	295	10	3.9	3.0/6.5	1.0	270	62	20,380	19,900	1.66	56	0.23
E4	231	15	6.3	3.0/6.0	1.0	330	65	17,250	18,410	1.62	62	0.23
E5	320	10	3.0	6.5/6.1	0.6	330	40	13,520	12,580	2.15	80	0.44
E6	321	10	3.0	7.5/7.2	1.0	300	24	8070	6100	1.67	40	0.43
E7	323	10	2.9	3.0/5.0	0.2	420	78	27,220	25,000	1.46	41	0.18
E8	262	30	13.7	3.0/6.9	1.0	330	80	23,000	23,530	1.63	79	0.23
E9	485	10	1.9	3.0/4.9	0.2	390	75	38,280	30,000	1.61	39	0.21
E10	323	20	5.7	3.0/4.8	0.2	540	86	29,700	24,100	1.50	48	0.27
E11	215	10	4.3	3.0/4.9	0.2	510	75	18,500	19,000	1.45	35	0.15
E12[e]	516	20	2.9	5.0/5.0	-	600	85	74,150	76,300	1.60	65	0.28

[a] [CTA]/[initiator] ratio keeps at 5 : 1, the polymerization temperature was 70°C and KPS used as the initiator for **E1–E4,** the polymerization temperature was 50°C and VA044 used as the initiator for **E5–E12**.
[b] Mass percent of monomers to the total feeding mass.
[c] D_z (average diameter) and σ (polydispersity factor) were determined by dynamic light scattering analysis. σ value closed to zero indicated the narrow distribution of latex particles.
[d] The latex was unstable and partially coagulated, upside M_n corresponds to polymer in latex and downside M_n to coagulated polymer.
[e] Seed emulsion polymerization of styrene in the presence of entry **E7** final emulsion as seeds.

Effect of Neutralization on *Ab Initio* Emulsion Copolymerization of VDC and MeA

The emulsion copolymerizations of VDC and MeA were performed using neutralized PAA–TTCA (entry **E1**), un-neutralized (entry **E2**), and neutralized PAA-*b*-PS-TTCA (entries **E3–E11**) as the CTAs and the emulsifiers. The polymerizations were performed under various conditions shown in Table I to evaluate the efficiency of macro-RAFT agent for the emulsion copolymerization of VDC and MeA.

Effect of Macro-RAFT Agent Structure. First, the emulsion copolymerization was performed using the neutralized PAA–TTCA (with an initial pH of about 6.0) as the CTA and the emulsifier, which has been proved as an efficient macro-RAFT agent for the preparation of PAA-*b*-PBA diblock copolymers.[28] The stable latex with a *Z*-average latex particle size of 78 nm was obtained. As shown in Figure 2, the molar mass of copolymer was increased significantly compared with that of PAA–TTCA, while the molecular weight distribution became wider (PDI = 3.62) after the copolymerization, indicating the decreased controllability of the emulsion polymerization system. This may be ascribed to the high water solubility of the leaving/initiating radicals of PAA-based sodium salt. VDC is slightly soluble in water (0.23–0.30 wt %).[29] After VDC monomer was initiated by the primary radicals in aqueous phase, the VDC oligomer radicals would enter the micelles of the PAA-based macro-RAFT agent. Because of the fast transfer reaction, the leaving group of CTA was prone to desorb into the aqueous phase and could not initiate the monomer in the micelles. The desorbed radicals may either terminate in the aqueous phase or enter another micelle after the addition reaction with the VDC units. The initial radicals formed from PAA-*b*-PS have lower solubility in water and may have higher probability of reinitiating than exit upon transfer. So, the PAA-*b*-PS-TTCA macro-RAFT agent was used in the following emulsion polymerizations.

Effect of Neutralization of PAA-*b*-PS-TTCA Macro-RAFT Agent on Colloidal Stability. It was reported that the neutralization of PAA-*b*-PS-TTCA macro-RAFT agent played a key role in the *ab initio* RAFT emulsion polymerization of St or butadiene.[30] The influences of neutralization degree and method of PAA-*b*-PS-

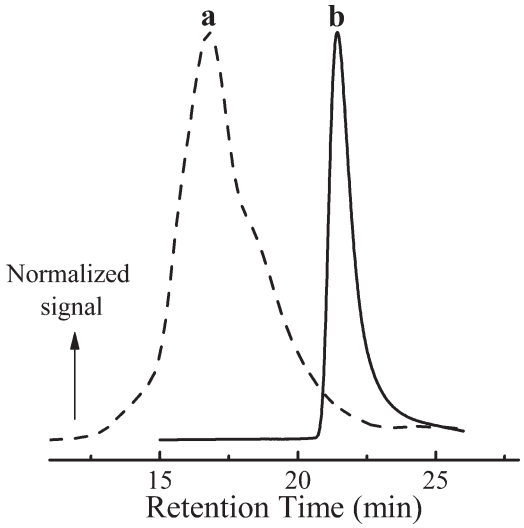

Figure 2. GPC traces of PAA-*b*-PVDC copolymer (a) and PAA–TTCA macro-RAFT agent (b).

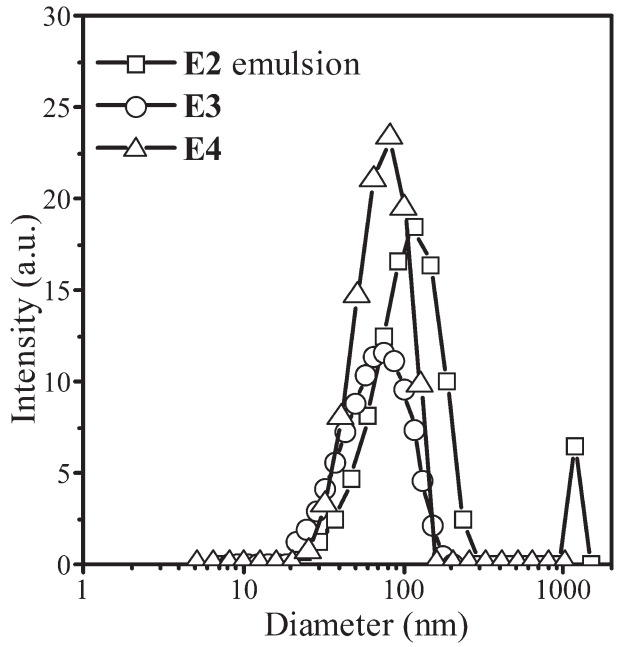

Figure 3. Particle size distributions of VDC copolymer latexes prepared by RAFT emulsion polymerizations with different neutralization method. Entry **E2**, no neutralization; entry **E3**, entry **E4**, post-neutralization.

TTCA macro-RAFT on the controllability of polymerization and the characteristic of resulted latex were investigated in entries **E2–E8**, as shown in Table I. In entry **E2**, no NaOH was added throughout the polymerization and the latex coagulated after polymerization, in which the coagulum was 10 wt % relative to the total polymer mass. As shown in Table I, the measured molecular weights of VDC copolymers taken from the stable latex and coagulum were similar, indicating that the coalescence of latex particles occurred at the later stage of polymerization. In entry **E3** and entry **E4**, NaOH solution was added after 60 min of polymerization and no coagulum was detected in the resulted latex.

The particles size distributions and TEM micrographs of VDC copolymer latexes prepared in entries **E2**, **E3**, and **E4** are shown in Figures 3 and 4, respectively. The particle size distributions are monomodal for entries **E3**, **E4**, but bimodal for entry **E2**, in agreement with the TEM results. It can be seen that the particle size and polydispersity index of entry **E2** emulsion are much greater than that of entries **E3**, **E4** emulsion, which further demonstrates the occurrence of coalescence due to the decreased colloidal protection to the latex particles as the particle size and interfacial area increased.

In entry **E5** and entry **E6**, NaOH solution was added before the emulsion polymerization ($[OH^{-1}]/[—COOH]$ ratio at 0.6 and 1.0, respectively). Because of the H^+ originated from the decomposition of KPS, the final latex using KPS as the initiator has low pH value than that using VA044 as the initiator at the same $[OH^{-1}]/[—COOH]$ ratio. The difference between these two experiments was that NaOH was over dosage for neutralization of carboxyl acid groups of PAA-*b*-PS-TTCA in entry **E6**. The particles size distributions of the latexes prepared in entry **E5** and entry **E6** are shown in Figure 5. It can be seen that particle sizes are not uniform and the particle distributions are broader. Furthermore, a smaller particle size of the entry **E6** latex than the entry **E5** latex may attribute to lower interface tension at high pH case. Considering the low polymerization conversions of entry **E5** and entry **E6** polymerizations, the colloidal stabilities of latexes obtained were low.

Similar to the entry **E3**, NaOH solution was also added after the polymerization for 60 min in entry **E7**. From the particle size distribution curves shown in Figure 5 and TEM micrographs shown in Figure 6, it can be seen that the particle size distribution is monomodal and narrow for entry **E7**. In entry **E8**, the monomer mass percentage was increased to be 30% and NaOH was added after 60 min of polymerization, the obtained latex had a good colloidal stability and a narrow particle size distribution as shown in Figures 5 and 6.

Effect of Neutralization of PAA-*b*-PS-TTCA Macro-RAFT Agent on Kinetics and Controllability of Polymerization. By comparing the polymerization kinetics of entry **E6** and entry **E7** shown in Figure 7, it can be seen that a significant retardation of polymerization occurred and the final conversion of monomer was lower in entry **E6** as the PAA-*b*-PS-TTCA macro-RAFT agent neutralized with $[OH^{-1}]/[—COOH]$ ratio of 1.0. This may be caused by the radical desorption due to the increased hydrophilicity of the leaving group of unreacted macro-RAFT agents. These hydrophilic radical may terminate in aqueous phase with increased pH and cause the low conversion. With post-neutralizing and $[OH^{-1}]/[—COOH]$ ratio at 0.6 in entry **E7**, no obvious induction period was observed and a high conversion of monomers (*ca.* 70%) was achieved after the polymerization for 150 min.

The GPC curves of entries **E5–E8** were shown in Figure 8. Entry **E5** and entry **E6** showed the bimodal molecular weight distribution, while entry **E7** and entry **E8** exhibited the unimodal distribution. This further confirmed that the post-neutralization of RAFT agent offered a better controllability of polymerization.

Therefore, for VDC RAFT emulsion polymerization systems initiated by KPS or VA044, post-neutralization of PAA containing block copolymers and keeping $[OH^{-1}]/[—COOH]$ ratio at 0.2–1.0 are recommended to obtain PVDC latex with high polymerization rate, good colloidal stability, and well controllability of molecular structures.

Kinetics and Particle Formation Mechanism of RAFT Emulsion Copolymerization of VDC and MeA

On the basis of the aforementioned results, the kinetics of *ab initio* emulsion polymerization were investigated using PAA-*b*-PS-TTCA as the CTA and VA044 as the initiator at 50°C, in which NaOH was added to adjust pH value to 5 after polymerizing for 60 min (entries **E7**, **E9–E11**). In all cases, the RAFT emulsion polymerization of VDC was much faster than RAFT solution polymerization reported previously.[19,21] A conversion greater than 70% could be achieved after polymerizing for 300 min.

Furthermore, the initial amount of macro-RAFT agent was varied from 1.9 mmol L_{aq}^{-1} (entry **E9**), to 2.9 mmol L_{aq}^{-1} (entry

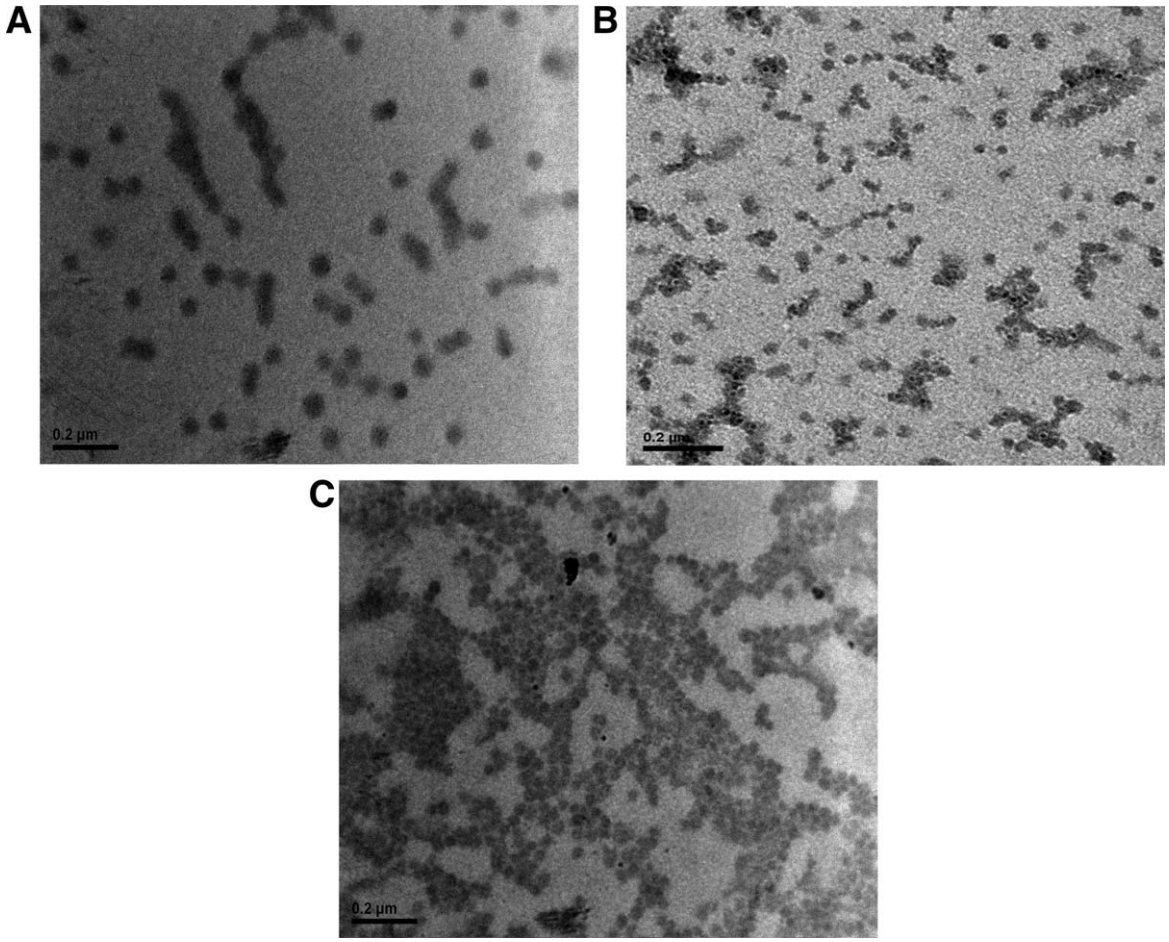

Figure 4. TEM micrographs of VDC copolymer latexes prepared by RAFT emulsion polymerizations with different neutralization policy (A) **E2**, (B) **E3**, and (C) **E4**.

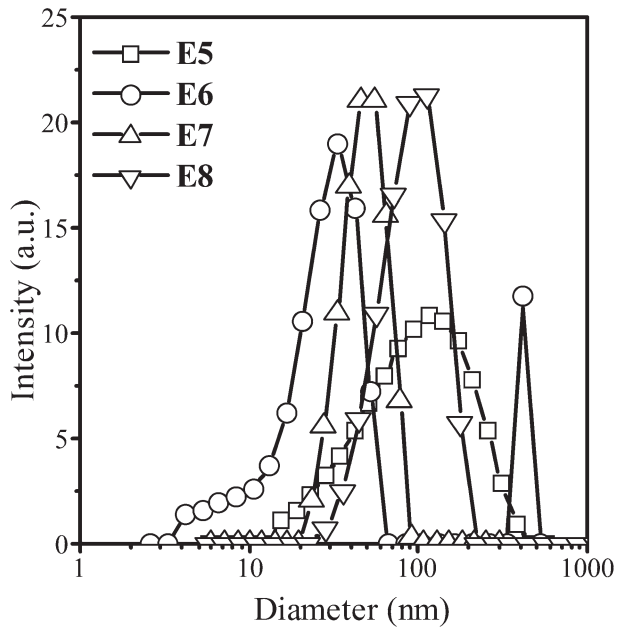

Figure 5. Particle size distributions of VDC copolymer latexes prepared by RAFT emulsion polymerizations using use VA044 as initiator.

E7) and finally 5.7 mmol L_{aq}^{-1} (entry **E10**). As shown in Figure 9, the polymerization rate was increased with the increasing amount of macro-RAFT agent. This might be ascribed to the dependence of polymerization rate on the number of micelles and latex particles. The PAA-*b*-PS-TTCA was used not only as a RAFT agent but also as a stabilizer in emulsion polymerization. More micelles and latex particles would be formed as the usage of the RAFT agent increased. Therefore, the polymerization rate would be increased. The entry **E10** latex had a higher solid content than the entry **E7** latex, while the ratios between $[M]_0$ and $[CTA]_0$ of entry **E7** and entry **E10** were same. Thus, they almost had the same polymerization rate due to the near number of latex particles.

Variations of the number-average molar masses (M_n) and PDIs of PVDC with the monomer conversion are shown in Figure 10. It can be seen that the experimental M_n values of all cases were increased continuously and in good agreement with the corresponding theoretical values, indicating a complete consumption of macro-RAFT agent. The PDI values were significantly decreased after the nucleation stage, evidencing a well controllability of the RAFT agent to the polymerization process.

The GPC trace of PVDC prepared in entry **E7** is shown in Figure 11. It can be seen that the GPC traces change from the

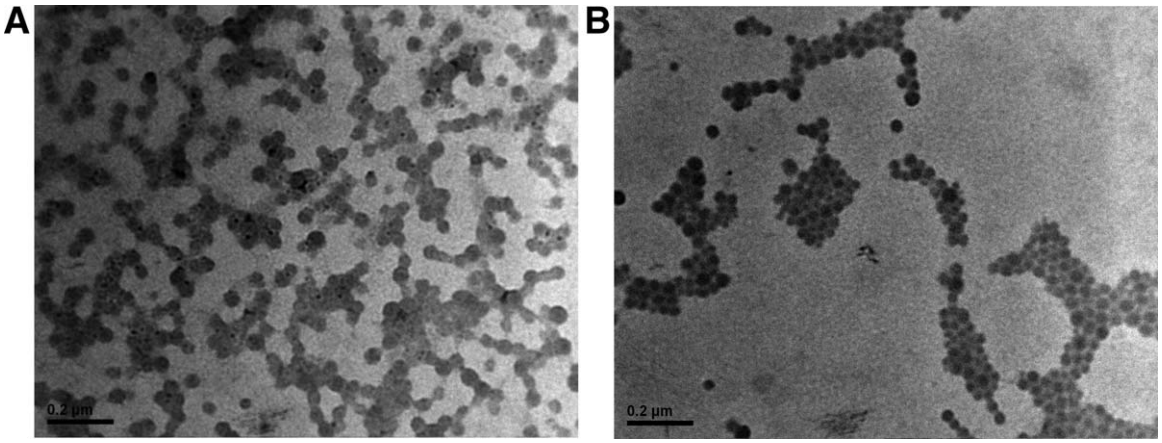

Figure 6. TEM micrographs of VDC copolymer latexes prepared by RAFT emulsion polymerization using VA044 as initiator (A) entry **E7**; (B) entry **E8**.

bimodal to unimodal distribution as the polymerization conversion increased, which demonstrated that the macro-RAFT agent was consumed quickly and only a small percentage remained at the end of polymerization.

The above results also indicated a well controllability of the VDC emulsion polymerization mediated with post-neutralized PAA-*b*-PS-TTCA macro-RAFT agent.

The variations of latex particle sizes with conversion for entries **E7**, **E9–E11** are shown in Figure 12. Because of the presence of monomer droplets, the particles size was greater at the early stage of polymerization. The particle sizes and polydispersities were significantly decreased as conversion increased at the lower conversion stage (<10%), and changed slightly between 30 and 60% conversion. As the conversion exceeded 60%, the particle sizes and polydispersities were slightly increased. The particle sizes of the final latexes were consistent with the particles size observed in TEM micrographs (shown in Figure 6).

It is interesting that the critical conversion (about 30%), at which the particle size tends to be constant, is much lower than the conventional emulsion polymerization of vinylidene chloride (60%).[31] It may be caused by improved swelling ability of monomers in the VDC polymer containing MeA,[32] which is also confirmed in the conventional emulsion copolymerization of VDC and methyl methacrylate by Nomura et al.[11]

Taking the entry **E9** as an example, TEM micrographs and the size distributions of the latex particles obtained at different conversions are shown in Figures 13 and 14, respectively.

At a low conversion (<10%), the latex exhibits a broad (16–850 nm) and multi-modal particle size distribution, which agrees

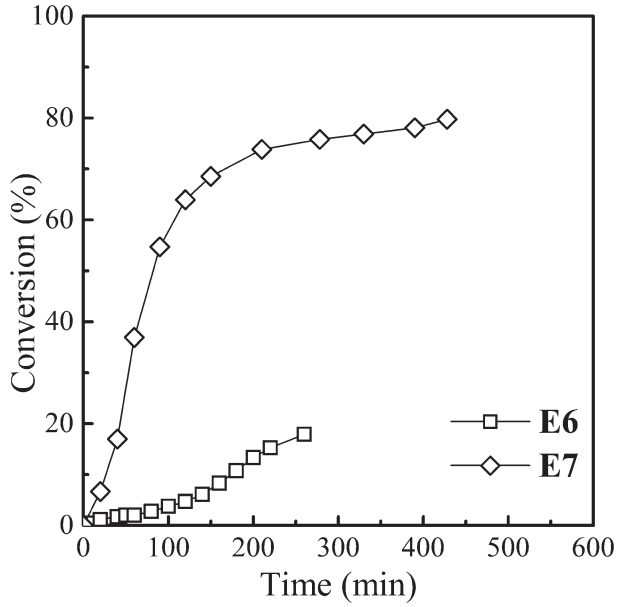

Figure 7. Conversion versus time curves of RAFT emulsion polymerization of VDC mediated by initially (entry **E6**) and post-neutralized PAA-*b*-PS-TTCA (entry **E7**).

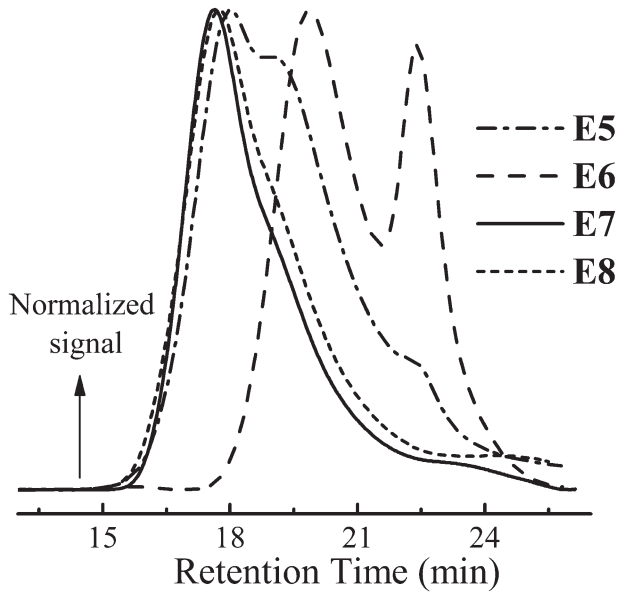

Figure 8. GPC trace of VDC copolymers prepared via RAFT emulsion polymerizations mediated by previous neutralized (entries **E5** and **E6**) and post neutralized PAA-*b*-PS-TTCA (entries **E7** and **E8**).

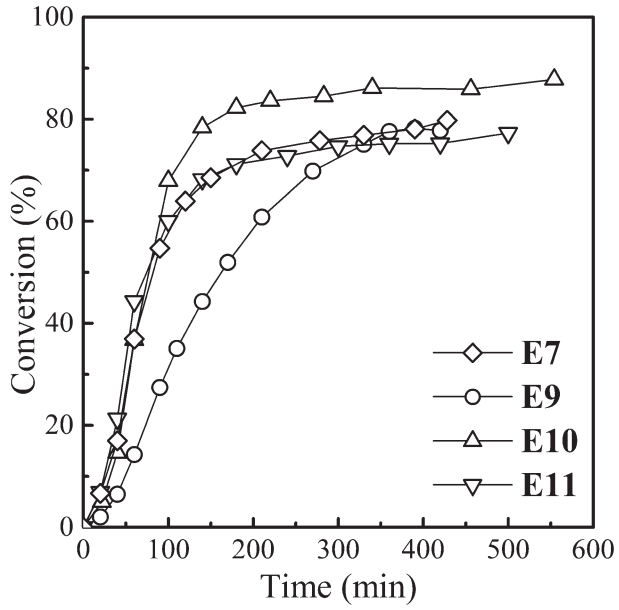

Figure 9. Conversion versus time curves of RAFT emulsion polymerization of VDC mediated by neutralization PAA-*b*-PS-TTCA and used VA044 as initiator.

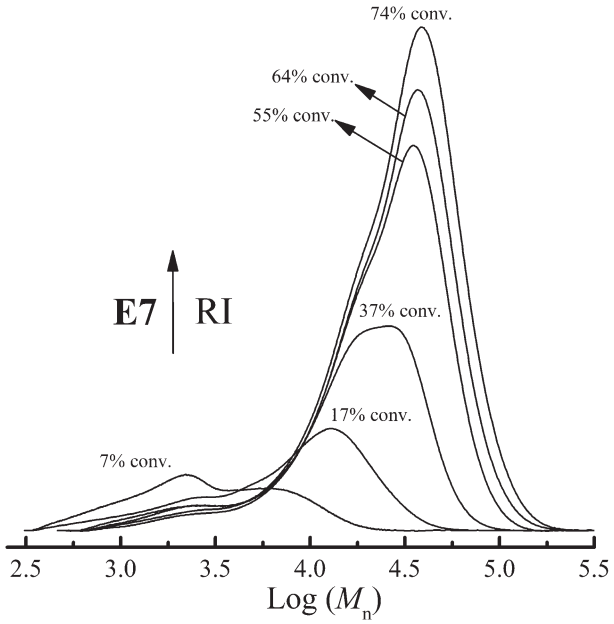

Figure 11. Evolution of GPC traces with monomer conversion for RAFT emulsion polymerization of VDC mediated by post-neutralized PAA-*b*-PS-TTCA as macro-RAFT agent.

with the characteristic of a nucleation stage of the emulsion polymerization. As the conversion increased to be 27%, the latex shows a monomodal particle size distribution ranging from 20 to 100 nm. As high conversions (60 and 76%), the particle size of the latex is slightly increased. Because of the decreased colloidal protection caused by the increase of the particles size and interfacial area, and low film formation temperature of PVDC latex, a slight coalescence of the latex particles could be seen from TEM micrographs.

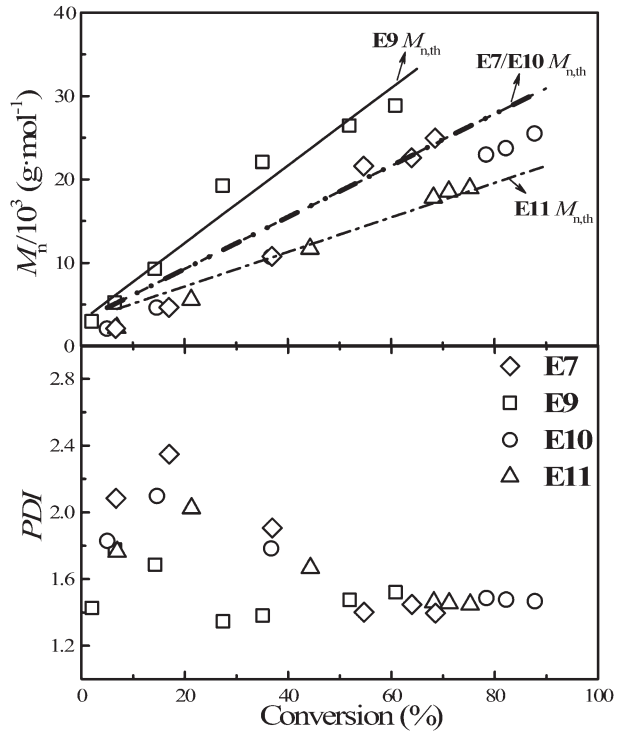

Figure 10. Variations of M_n and PDI with monomer conversion for RAFT emulsion polymerization of VDC mediated by post-neutralized PAA-*b*-PS-TTCA; (—) theoretical M_n.

In sum, *ab initio* RAFT emulsion polymerization of VDC showed a greater polymerization rate and better control over molar mass than solution polymerization. The resulted latex has a good colloidal stability and narrow particle size distribution, which would facilitate this surfactant-free emulsion polymerization process to prepare PVDC-based latexes with well structure design and no small surfactants in industrial scale.

Seeded Emulsion Polymerization of Styrene

Because the VDC copolymer latexes prepared in the aforementioned *ab initio* RAFT emulsion polymerization contained the living amphiphilic triblock PAA-*b*-PS-*b*-PVDC chains, they could be extended by another block to attain the novel block copolymers and nanostructured particles. Because of the high T_g of PS and its immiscibility with PVDC, styrene was chosen to prepare the block copolymer of PVDC. As shown in Table I, the seeded emulsion polymerization was investigated using the entry **E7** final emulsion latex as the seed, which had a solid content of 10% and a M_n^{GPC} of 25 kg mol^{-1}.

The GPC traces of the macro-RAFT agent, seeded VDC copolymer, and PAA-*b*-PS-*b*-PVDC-*b*-PS are shown in Figure 15. The shift of the GPC traces demonstrated the formation of PAA-*b*-PS-*b*-PVDC-*b*-PS copolymers ($M_n^{GPC} = 76.3$ kg mol^{-1}, PDI = 1.6).

DLS analyses showed that the PAA-*b*-PS-*b*-PVDC-*b*-PS latex exhibited a mono-modal particle size distributions

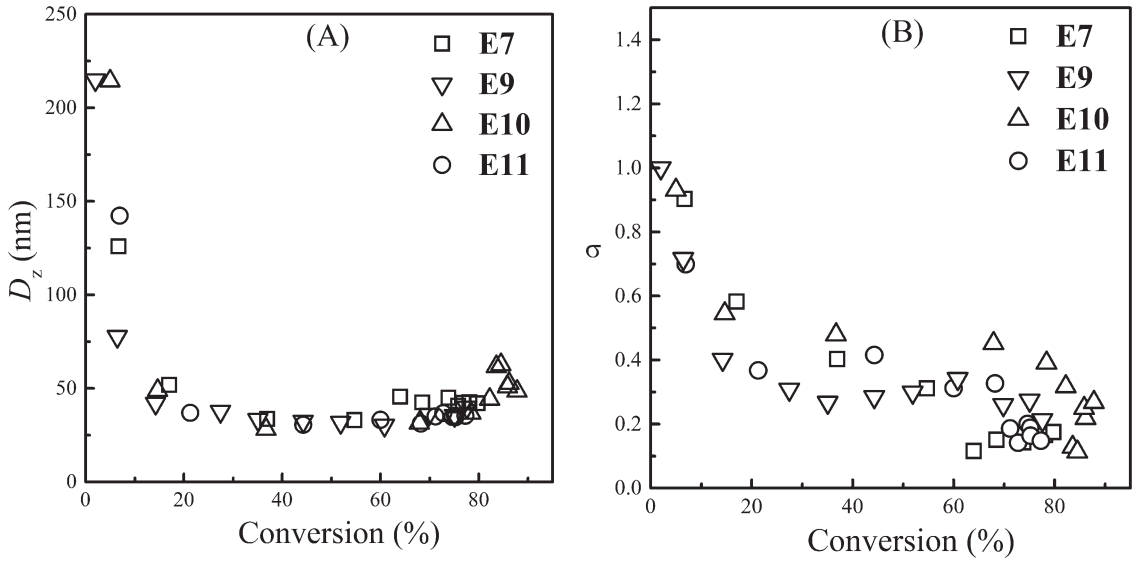

Figure 12. Variation of particle diameter (left A) and polydispersity factor (right B) with conversion for VDC emulsion polymerization mediated by post-neutralized PAA-*b*-PS-TTCA macro-RAFT agent.

($\sigma = 0.3$), and its size was grown from 40 nm of the seeds to 60 nm. The number of particles in the seeded PAA-*b*-PS-*b*-PVDC latex and PAA-*b*-PS-*b*-PVDC-*b*-PS copolymer latex were closed each other ($\approx 2 \times 10^{18}$ L^{-1}), which demonstrated that no secondary nucleation was taken place.

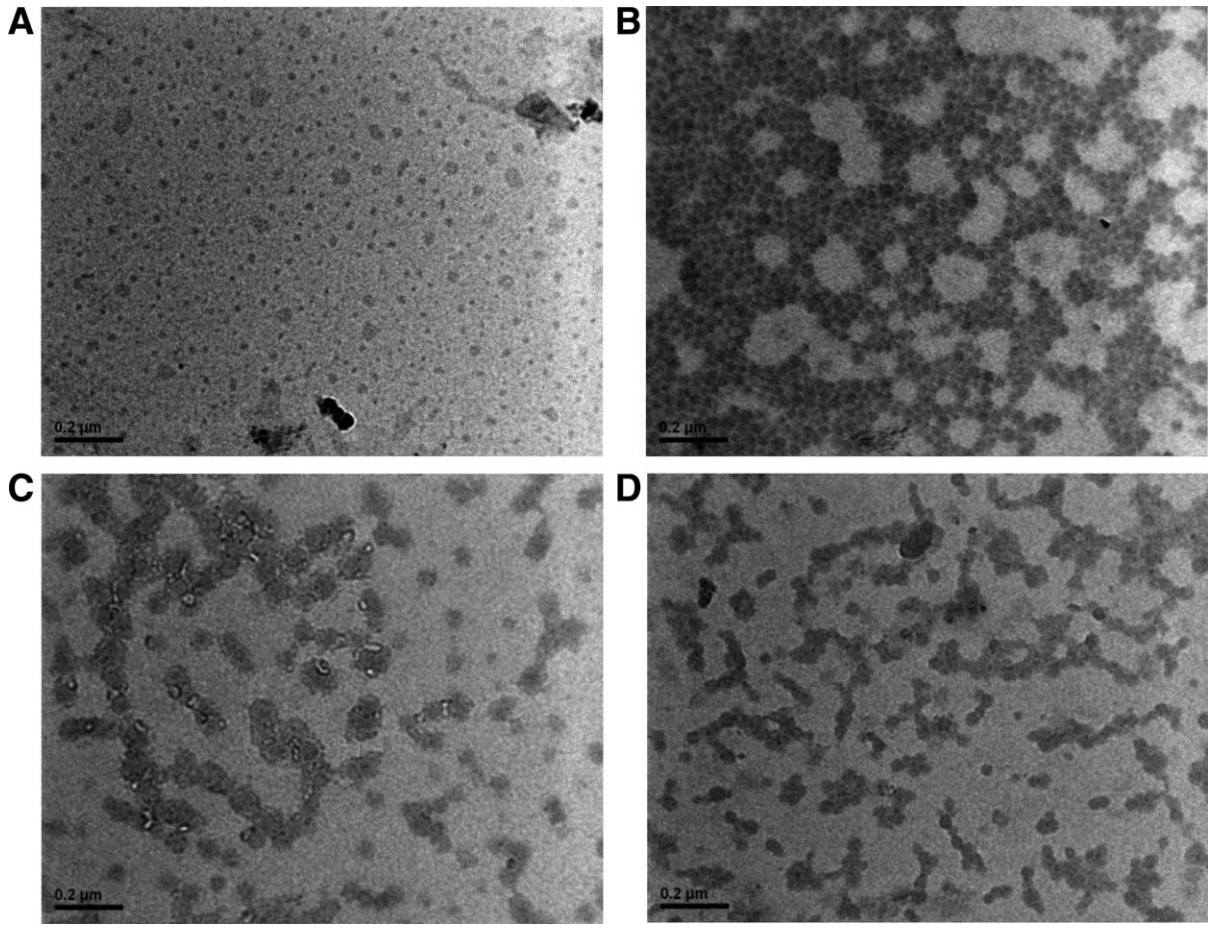

Figure 13. TEM micrographs of PVDC latexes with different conversions of entry **E9** RAFT emulsion polymerization (A) 6% conversion, (B) 27% conversion, (C) 60% conversion, and (D) 76% conversion.

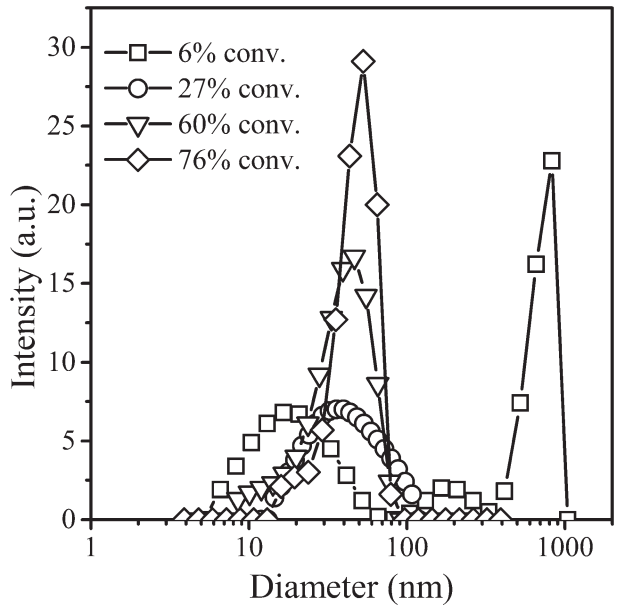

Figure 14. Particle size distributions of PVDC latexes with different conversions of entry **E9** RAFT emulsion polymerization.

The morphology of PAA-*b*-PS-*b*-PVDC-*b*-PS copolymer latex particles is shown in Figure 16. The film formation temperature of the latex was increased as PS incorporated into polymer chains. Thus, well separated particles with spherical shape could be clearly observed in TEM micro-graph.

The above results demonstrated the living character of the RAFT emulsion polymerization of VDC and the chain extension ability of PAA-*b*-PS-*b*-PVDC copolymers.

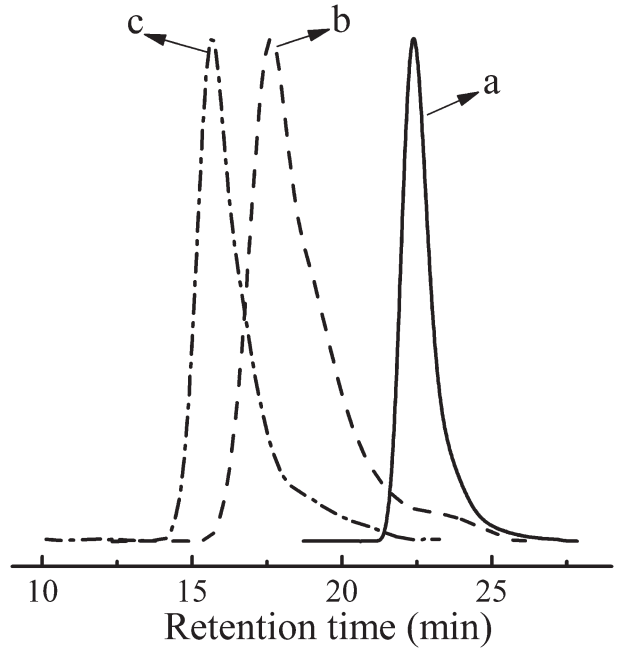

Figure 15. GPC traces for macro-RAFT agent (a), seeded PAA-*b*-PS-*b*-PVDC (b), and PAA-*b*-PS-*b*-PVDC-*b*-PS block copolymer (c).

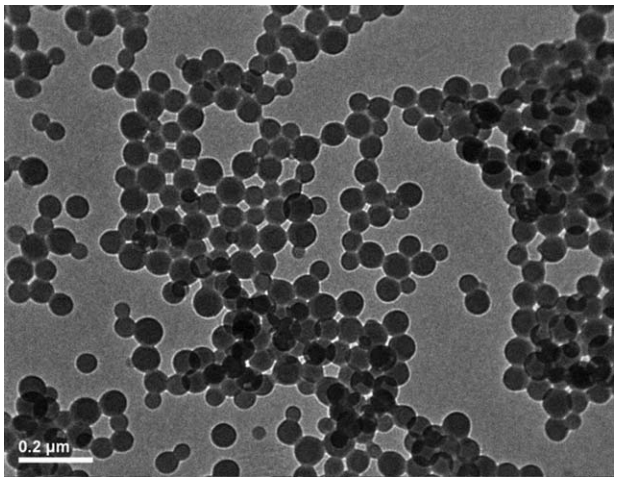

Figure 16. TEM micrograph of PAA-*b*-PS-*b*-PVDC-*b*-PS latex particles.

CONCLUSIONS

The emulsion copolymerizations of VDC and MeA were performed in the presence of the amphiphilic macro-RAFT agent (neutralized PAA–TTCA, PAA-*b*-PS-TTCA, or neutralized PAA-*b*-PS-TTCA) acted both as the RAFT agent and the colloidal stabilizer. The structure and the neutralization policy of macro-RAFT agents had great influences on the latex stability, the kinetics, and controllability of polymerization. The emulsion copolymerization was out of control as indicated by a great PDI of the resulted copolymer (=3.62) when previously neutralized PAA–TTCA was used. The polymerization rates were lower and the latexes were not stable when PAA-*b*-PS-TTCA or previously neutralized PAA-*b*-PS-TTCA was used as the RAFT agent. The well-controlled *ab initio* RAFT VDC emulsion polymerization can be achieved as PAA-*b*-PS-TTCA post-neutralized by adjusting $[OH^{-1}]/[-COOH]$ ratio at 0.2–1.0 after 60 min of polymerization. In this case, the emulsion polymerization is efficient and stable. The targeted degree of polymerization for the PVDC can be varied, indicating that the system is well controllable and tunable. Moreover, the process can be extended to the synthesis of multi-block copolymer particles, proving that high chain end functionality is maintained throughout the polymerization. By applying of the present emulsion polymerization method, PVDC and PVDC-based block copolymer latexes with well-defined structures and without small molecule surfactants can be prepared.

ACKNOWLEDGMENTS

This work was supported by National Natural Foundation of China (Grant no. 21176209).

REFERENCES

1. Grunlan, J. C.; Mehrabi, A. R.; Chavira, A. T.; Nugent, A. B.; Saunders, D. L. *J. Comb. Chem.* **2003**, *5*, 362.
2. Brown, R. A.; Budd, P. M.; Price, C.; Satgurunathan, R. *Eur. Polym. J.* **1993**, *29*, 337.
3. Howell, B. A.; Zhang, J. *J. Vinyl Addit. Technol.* **2006**, *12*, 88.

4. Hsieh, T. H.; Ho, K. S. *J. Polym. Sci.: Polym. Chem.* **1999**, *37*, 2035.
5. Collins, S.; Yoda, K.; Anazawa, N.; Birkinshaw, C. *Polym. Degrad. Stab.* **1999**, *66*, 87.
6. Garnier, J.; Dufils, P.; Vinas, J.; Vanderveken, Y.; van Herk, A.; Lacroix-Desmazes, P. *Polym. Degrad. Stab.* **2012**, *97*, 170.
7. Wessling, R. A.; Gibbs, D. S.; Obi, B. E.; Beyer, D. E.; Delassus, P. T.; Howell, B. A. *Kirk-Othmer Encycl. Chem. Technol.* **1999**, *25*, 691.
8. Gibbs, D. S.; Wessling, R. A.; Obi, B. E.; Delassus, P. T.; Howell, B. A. *Kirk-Othmer Encycl. Chem. Technol.* **1997**, *24*, 882.
9. Yu, Z.; Jia, H.; Li, B.; Li, B. *Polym. Int.* **1993**, *30*, 441.
10. Nomura, M.; Kodani, T.; Ojima, J.; Kihara, Y.; Fujita, K. *J. Polym. Sci.: Polym. Chem.* **1998**, *36*, 1919.
11. Nomura, M.; Sakai, H.; Kihara, Y.; Fujita, K. *J. Polym. Sci.: Polym. Chem.* **2002**, *40*, 1275.
12. Yuan, J.; Meng, J.; Kang, Y.; Du, Q.; Zhang, Y. *Appl. Surf. Sci.* **2012**, *258*, 2856.
13. Liu, H.; Zhang, Y.; Hu, J.; Li, C.; Liu, S. *Macromol. Chem. Phys.* **2009**, *210*, 2125.
14. Patil, Y.; Ameduri, B. *Polym. Chem.* **2013**, *4*, 2783.
15. Jennings, J.; Beija, M.; Richez, A. P.; Cooper, S. D.; Mignot, P. E.; Thurecht, K. J.; Jack, K. S.; Howdle, S. M. *J. Am. Chem. Soc.* **2012**, *134*, 4772.
16. Sienkowska, M. J.; Percec, V. *J. Polym. Sci.: Polym. Chem.* **2009**, *47*, 635.
17. Yang, D.; Feng, C.; Hu, J. *Polym. Chem.* **2013**, *4*, 2384.
18. Severac, R.; Lacroix-Desmazes, P.; Boutevin, B. *Polym. Int.* **2002**, *51*, 1117.
19. Rixens, B.; Severac, R.; Boutevin, B.; Lacroix-Desmazes, P. *J. Polym. Sci.: Polym. Chem.* **2006**, *44*, 13.
20. Warnant, J.; Garnier, J.; van Herk, A.; Dufils, P.-E.; Vinas, J.; Lacroix-Desmazes, P. *Polym Chem.* **2013**, *4*, 5656.
21. Velasquez, E.; Pembouong, G.; Rieger, J.; Stoffelbach, F.; Boyron, O.; Charleux, B.; Agosto, F. D.; Lansalot, M.; Dufils, P.; Vinas, J. *Macromolecules* **2013**, *46*, 664.
22. Rieger, J.; Stoffelbach, F.; Bui, C.; Alaimo, D.; Jérôme, C.; Charleux, B. *Macromolecules* **2008**, *41*, 4065.
23. Ferguson, C. J.; Hughes, R. J.; Nguyen, D.; Pham, B. T. T.; Gilbert, R. G.; Serelis, A. K.; Such, C. H.; Hawkett, B. S. *Macromolecules* **2005**, *38*, 2191.
24. Wang, X.; Luo, Y.; Li, B.; Zhu, S. *Macromolecules* **2009**, *42*, 6414.
25. Wei, R.; Luo, Y.; Xu, P. *J. Polym. Sci.: Polym. Chem.* **2011**, *49*, 2980.
26. Xu, S.; Huang, J.; Xu, S.; Luo, Y. *Polymer* **2013**, *54*, 1779.
27. Lai, J. T.; Filla, D.; Shea, R. *Macromolecules* **2002**, *35*, 6754.
28. Chenal, M.; Bouteiller, L.; Rieger, J. *Polym. Chem.* **2013**, *4*, 752.
29. DeLassus, P. T.; Schmidt, D. D. *J. Chem. Eng. Data* **1981**, *26*, 274.
30. Chen, Y.; Luo, W.; Wang, Y.; Sun, C.; Han, M.; Zhang, C. *J. Colloid Interf. Sci.* **2012**, *369*, 46.
31. Wiener, H. *J. Polym. Sci.* **1951**, *7*, 1.
32. Obi, B. E.; DeLassus, P. T.; Howell, B. A.; Dangel, B. *J. Polym. Sci.: Polym. Phys.* **1995**, *33*, 2019.